JOURNAL of
MATERIALS and MECHATRONICS:A

e-ISSN 2717-8811
JournalMM, 2025, 6(1), 32-48
https://doi.org/10.55546/jmm.1590391

Araştırma Makalesi / Research Article

Comprehensive Design and Testing of a BLDC Motor for Direct Drive EV Applications

Mücahit SOYASLAN[1*], Mohamad BAZAZIAN[2], Osman ELDOĞAN[3]

[1*] Sakarya University of Applied Sciences, Faculty of Technology, Department of Mechatronics Engineering, Sakarya, Türkiye, ORCID ID: https://orcid.org/0000-0001-6658-5169, msoyaslan@subu.edu.tr
[2] Sakarya University of Applied Sciences, Faculty of Technology, Department of Mechatronics Engineering, Sakarya, Türkiye, ORCID ID: https://orcid.org/0000-0003-2881-958X, mohamad.bazazian@ogr.sakarya.edu.tr
[3] Sakarya University of Applied Sciences, Faculty of Technology, Department of Mechatronics Engineering, Sakarya, Türkiye, ORCID ID: https://orcid.org/0000-0001-9236-8985, eldogan@subu.edu.tr

Geliş/ Received: 24.11.2024; **Revize/Revised:** 24.12.2024 **Kabul / Accepted:** 14.01.2025

ABSTRACT: This paper proposes a 2 kW in-wheel brushless direct current (BLDC) motor design for a light electric vehicle (EV). The EV is designed for a predefined route in electric vehicle races. The BLDC motor was directly mounted into the vehicle's wheel rim. Initially, dynamic model of EV was calculated according to vehicle characteristics. The motor's slot/pole ratio was selected as 36/32. The designs for the stator, rotor, and magnets were subsequently developed based on the motor's boundary dimensions, aiming for low cogging torque and high efficiency. To achieve this, the distance between stator tooth tips was optimized. The design was validated through 2D finite element analyses, followed by the motor's production. Performance tests conducted with the experimental setup confirmed that the design matches the experimental results.

Keywords: Electric vehicle, BLDC motor, Electric motor design, Outer rotor, EV dynamic model

*Sorumlu yazar / Corresponding author: msoyaslan@subu.edu.tr
Bu makaleye atıf yapmak için /To cite this article

Soyaslan, M., Bazazian, M., Eldoğan, O. (2025). Comprehensive Design and Testing of a BLDC Motor for Direct Drive EV Applications. Journal of Materials and Mechatronics: A (JournalMM), 6(1), 32-48.

1. INTRODUCTION

Electric vehicles (EVs) have begun to replace internal combustion vehicles in today's world. Various companies engaged in this sector focus on designing high efficiency EVs. Various battery packs and electric motors are used in these vehicles. Permanent Magnet Synchronous Motors (PMSMs) typically find application in larger electric or hybrid vehicles, whereas BLDC motors are favoured for smaller light EVs. Light EVs are typically scooters, small cars or cargo bikes with a carrying capacity of 50-100 kg and a speed of 25-50 km/h (Soyaslan, 2023).

BLDC motors used in light EVs can be classified into two types based on their structure: radial flux and axial flux. The studies conducted compare radial and axial flux motors in terms of efficiency, cost, and volume. Radial flux motors are further classified into two types: internal and outer rotor designs. While internal rotor motors are utilized in certain applications to transfer motion, outer rotor designs also referred to as in-wheel motors are the preferred choice for direct wheel drive applications. In outer rotor EV designs, parameters such as slot/pole ratio, axial length, winding structures, magnet type, and thickness are generally optimized (Cabuk et al., 2019; Chawrasia et al., 2020; Cagıslar et al., 2020; Akar et al., 2021; Aliyadin et al., 2022; Ozupak, 2022; Tosun and Serteller, 2022; Soyaslan, 2023).

Rotor and stator designs and the effects of single or double rotors and stators on performance have been investigated (Zuki et al. 2020; Lee et al, 2020; Vadde and Sachin, 2021; Hussain et al. 2021). Studies have been carried out to minimize cogging torque and torque fluctuation for more vibration-free and comfortable motors. In these studies, various pole embraces (ratio of magnetic pole arc to pole pitch), skewing stator or rotor laminations technique, and various magnet shapes, and various control techniques were used (Ocak et al., 2016; Soyaslan et al., 2019; Minh et al., 2021; Rupam and Marwaha, 2021; Anuja and Doss, 2021; Anuja et al., 2022; Ozupak and Cinar, 2023).

In this paper, 2 kW outer rotor BLDC motor with 36/32 slot-pole was designed for a light EV. Distance between stator tooth tips (B_{s0}) was optimized for minimizing cogging torque. Parametric optimization method was used for achieving the optimum B_{s0} value. This study aims to reduce cogging torque by focusing on the distance between stator tooth tips, demonstrating that cogging torque minimization is possible without the need for the complex operations used in previous studies. The current density and magnetic flux density (B) values were kept below 4-5 A/mm^2 and 1.6 Tesla, respectively. In addition, stator slot fill factor value was selected below 50% for a more suitable winding. The motor design was validated after analytical and electromagnetic analyses. Prototype motor was produced and tested in the test setup and EV, confirming that the analysis results aligned with the test outcomes.

2. MATERIALS AND METHODS

2.1 Dynamic Model of EV

The EV's characteristics for racetrack conditions with low angle of slope were computed. Table 1 summarizes the vehicle parameters used based on track conditions. Racetrack view can be seen from Figure 1. The track is 1.950 km long, 10-12 meters wide and designed to turn clockwise. The total number of bends on the track is 9, 4 on the right and 5 on the left, and the highest longitudinal slope on the track is 1%. The selection of parameters, including slope angle and acceleration values, is based on typical driving conditions in electric vehicle races. The goal is to achieve the desired acceleration values, power output, and high motor efficiency based on the maximum slope angle on the race track and vehicle dynamics.

Table 1. EV characteristics.

Parameter	Value
Total mass, M (kg)	210
Rolling resistance coefficient, C_{rr}	0.007
Air density, ρ (kg/m^3)	1.2
Drag coefficient, C_d	0.3427
Frontal area, A (m^2)	1.29
Velocity of vehicle, V (m/s)	12.5
Acceleration, a (m/s^2)	0.12
Tire radius, r (m)	0.2921
Surface slope angle, θ (°)	1.2
Gravity acceleration, g (m/s^2)	9.81

Figure 1. EV racetrack view

The dynamic model of the vehicle is shown in Figure 2. The maximum torque requirement for an EV arises during full-load conditions on an inclined road, particularly when accelerating from zero speed to its nominal speed. The torque calculations for the BLDC motor are based on the torque required to achieve this acceleration, considering the maximum incline values of the race track. According to EV's dynamic model, traction force F_t and BLDC motor's output torque T_m was calculated. Three different forces acting on the vehicle in the opposite direction of movement are expressed in (1-3) (Soyaslan, 2023; Krasopoulos et al., 2017). These forces are aerodynamic resistance F_{ar}, rolling resistance F_{rr} and weight component of EV along sloped surface F_{ws}. F_{ar} force is calculated at the nominal speed of the vehicle which is taken 45 km/h (12.5 m/s). Tire radius is 23 inch, rotational speed and angular velocity are 408.6 rpm and 42.8 rad/s respectively. According to Newton's second law for the dynamic model of the EV, F_t was calculated with (4) as 124.2 N. Consequently, the required torque value (T_m) for the vehicle to move at the desired nominal speed has been calculated from (5) as 36.28 Nm, and the power value (P_{out}) has been calculated from (6) as 1552 W. Since the slope angles of different tracks are greater and the acceleration can be bigger, the output power value P_{out} has been updated to 2000 W and the rotational speed (N) to 526.42 rpm to achieve the desired speeds. Thus, the designed motor will be able to provide the desired torque even on high slope angle roads and with bigger acceleration values.

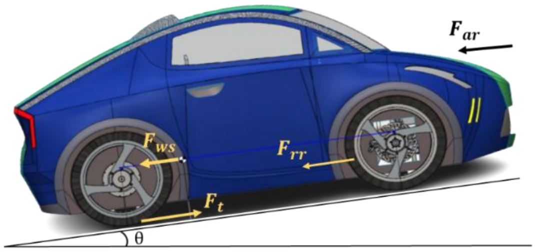

Figure 2. Dynamic model of the EV

$$F_{ar} = \frac{1}{2}\rho A C_d V^2 \tag{1}$$

$$F_{rr} = C_{rr} mgcos(\theta) \tag{2}$$

$$F_{ws} = mgsin(\theta) \tag{3}$$

$$M.a = F_t - F_{ar} - F_{rr} - F_{ws} \tag{4}$$

$$T_m = F_t r \tag{5}$$

$$P_{out} = T_m \omega \tag{6}$$

2.2 Outer Rotor BLDC Motor Design

The output torque expression for motor basic sizing is used as given in (7). Here, k is a constant, D is the air gap diameter, and L is the motor length. The region where rotational force is generated in motors is the air gap zone, where the interaction between the stator and rotor occurs. For inner rotor motors, the rotor diameter is generally used for D in the equation, while for outer rotor motors, the air gap diameter (D_{ag}) or stator outer diameter (D_{so}) is employed. In analytical motor calculations, the rotational speed in revolutions per second (*rps*, n) and the power per revolution (P_s) are obtained using (8) and (9), respectively. The air gap flux density (B_g) and specific electric loading (ac) values are selected from the graph in Figure 3 (Tosun and Serteller, 2022; Gürdal, 2001). The pole embrace value (α_m), representing the ratio of the magnetic pole arc to the pole pitch, is taken as 0.7. The average air gap flux density (B_{av}) and the motor output coefficient (C_o) are calculated using (10) and (11).

$$T_m = kD^2 L \tag{7}$$

$$n = \frac{N}{60} \tag{8}$$

$$P_s = \frac{P_{out}}{n} \tag{9}$$

$$B_{av} = B_g\, \alpha_m \tag{10}$$

$$C_o = \pi^2 B_{av}\, ac\, 10^{-3} \tag{11}$$

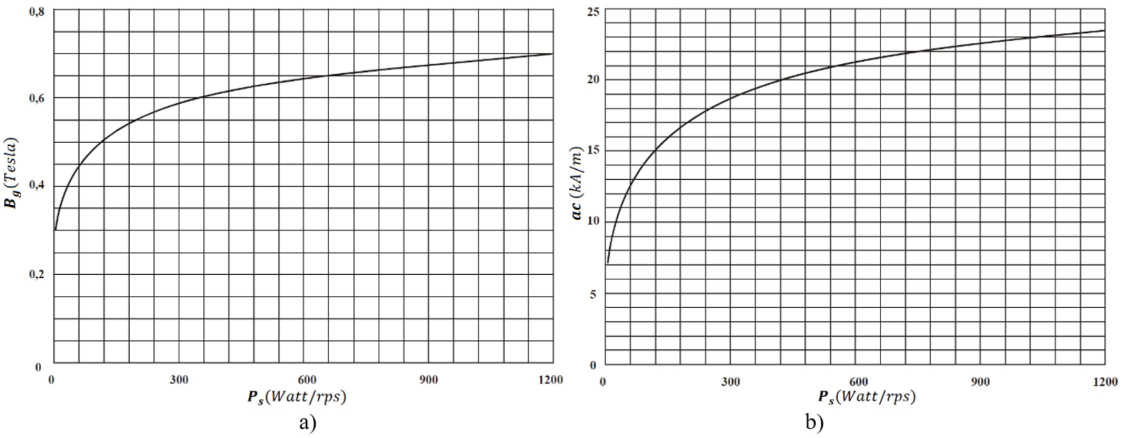

Figure 3. a) Power per round per second-Air gap flux density graph, b) Power per round per second-Specific electrical loading graph.

The volume of the motor's active components is closely related to $D_{ag}{}^2L$, and the rated torque is proportional to *Pout*/*n*. Therefore, the size-to-power relationship for an outer rotor BLDC motor is expressed using (12). According to this equation, the product of the motor stator diameter and length is determined. Subsequently, the motor's axial length to pole-pitch ratio (L/τ) must be defined. Various studies have examined this topic, selecting different ratios based on motor dimensions and power requirements. The pole-pitch ratio (τ) is calculated using (13), where *Np* represents the total number of poles. For surface-mounted brushless motors, τ values are typically chosen between 1 and 3 to minimize manufacturing costs (Murali et al., 2020). In this study, experiments with different τ values were conducted, ultimately deciding on τ = 3. The motor parameters derived from the given equations and selections are presented in Table 2. Based on these values, D_{ag} is calculated as 225.23 mm, and L as 66.33 mm. However, due to mechanical constraints and the requirement for EV installation, the axial length L was updated to 55 mm. The air gap thickness was set to 1 mm, considering manufacturing tolerances, and D_{so} was selected as 224 mm.

$$D_{ag}^2 L = \frac{P_{out} * 10^{-3}}{C_o n} \tag{12}$$

$$\tau = \frac{D_{ag}}{N_p} \tag{13}$$

Table 2. BLDC motor parameters

Parameter	Value
Output power, P_{out} (Watt)	2000
Pole number, N_p	32
Slot number, N_s	36
Round per minute, N (rpm)	526.42
Round per second, n (rps)	8.773
Power per round per second, P_s (watt/rps)	227.954
Airgap flux density, B_g (Tesla)	0.57
Specific electrical loading, ac (kA/m)	17200
Magnetic pole arc to pole pitch ratio, α_m	0.7
Average airgap flux density, B_{av} (Tesla)	0.399
Output coefficient value, C_o	67.733
Motor axial length to pole pitch ratio, L/τ	3

2.3 Dimensions and Cogging Torque Optimization

Fundamental sizing calculations were performed based on calculated values. After the basic sizing, parameter selections were refined through parametric testing. The stator slot dimensions were chosen to ensure sufficient space for windings and optimal flux flow. To reduce saturation in corner regions, radii were applied to the stator tooth tips. Excessively thick stator teeth narrow the slot area, reducing winding space, while overly thin teeth lead to saturation in the silicon steel. Therefore, the stator tooth width was selected to optimize magnetic flux density. The rotor core thickness was set to 11.25 mm, and the magnet thickness to 3.5 mm, aiming for the optimal thickness to produce the required torque. The magnets were embedded in slots created within the rotor using the wire erosion method, with a slot depth of 1.25 mm for secure magnet installation. The motor cross-sectional variables are shown in Figure 4, with their dimensions detailed in Table 3.

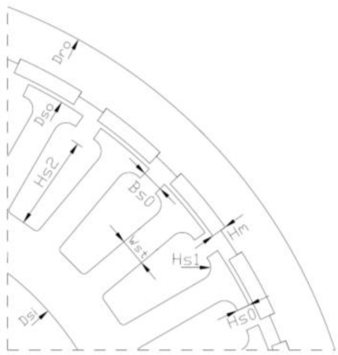

Figure 4. Dimensions of BLDC Motor

Table 3. BLDC motor dimension values

Motor Paremeter	Value
Stator outer diamater, D_{so}	224 mm
Stator inner diameter, D_{si}	145 mm
Rotor outer diamater, D_{ro}	253 mm
Stack length, L	55 mm
Magnet height, H_m	3.5 mm
Stator tooth width, W_{st}	6.3 mm
Tooth tip gap, B_{s0}	5 mm
Tooth tip height, H_{s0}	3 mm
Tooth tip Radius, H_{s1}	3 mm
Slot height, H_{s2}	21 mm

The reduction of cogging torque is essential to improve the efficiency and to reduce permanent magnet requirements of electric motors (Smolka and Nowacka, 2022; Jhankal, 2023). In the context of vibration and noise reduction, cogging torque has been identified as a significant factor affecting the smooth rotation of the rotor and the life of electric motors (Soyaslan et al., 2019, Kim et al., 2006). To minimize cogging torque and torque fluctuations in external rotor BLDC motors, various effective methods have been proposed in the literature. Adjusting the punching layout and applying placement irregularities in rotor magnets were used to reduce the cogging torque (Anuja and Doss, 2021; Leitner et al., 2019). Asymmetric magnets, step skewing and shifting angles have been experimentally applied to reduce harmonics of cogging torque (Doss et al., 2016; Avsar et al., 2024a). Optimizing BLDC motors by utilizing a skew angle on the stator or rotor core, along with enlarging the air gap, has shown significant reductions in cogging torque (Mandasari, 2023). Skewing the rotor and implementing a Halbach magnet array on the permanent magnet surface has been suggested to eliminate torque ripples and reduce cogging torque in permanent magnet BLDC motors (Minh et al., 2021). Additionally, adjusting slot and tooth widths, employing permanent magnet skewing, creating auxiliary teeth, using slot-less armatures, and incorporating notches in the rotor structure have been identified as effective methods to minimize cogging torque magnitude (Karthick et al., 2021). Furthermore, the reduction of cogging torque is crucial in direct-drive systems where there are no gears to minimize or absorb the cogging torque (Sarac, 2019). These methods play a crucial role in enhancing motor efficiency, reducing noise, and improving overall performance in a wide range of applications. In this study, stator tooth tip gap (B_{s0}) was selected as an optimization parameter for reducing the cogging torque. The objective function for the optimization was defined as the cogging torque, which the optimization sought to minimize. Parametric optimization method was used between 4-6 mm with 0.1 mm step. The parametric optimization results indicated that a B_{s0} value of 5 mm yielded one of the lowest cogging torque values. The optimized result is depicted in Figure 5.

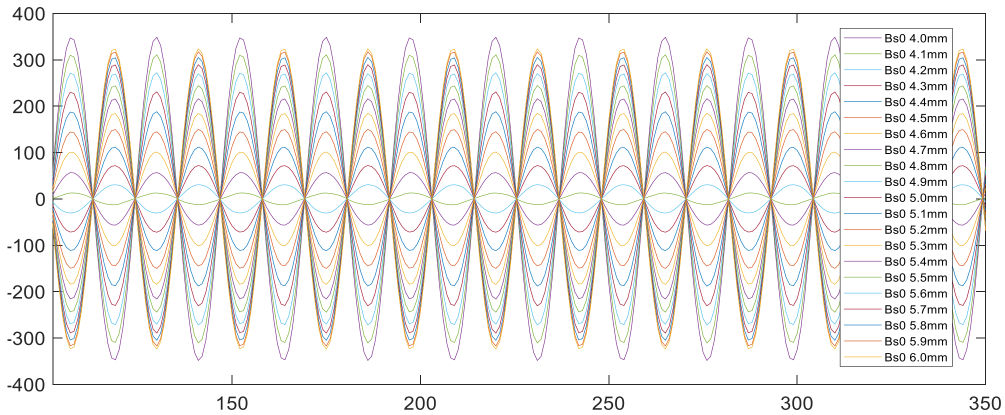

Figure 5. Cogging torque values regarding to B_{so} value

3. RESULTS AND DISCUSSION

3.1 Analyses Results

Electromagnetic analysis was conducted based on the specified stator and rotor dimensions. The winding scheme and hall effect sensors placement, derived using the Winding Scheme Calculator tool, are presented in Figure 6 (Niessen, 2019). A double-layer concentrated winding technique was applied to achieve high power density (Soyaslan, 2020).

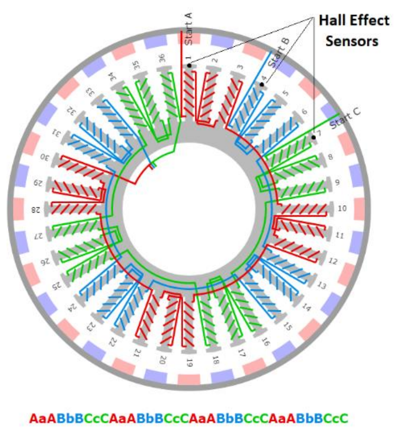

Figure 6. BLDC motor 36/32 Slot-Pole combination winding scheme

The electromagnetic transient analysis results obtained using Ansys Maxwell software are presented in Figures 7–9. Magnetic vector potential was used to determine the distribution and intensity of the magnetic field. A uniform distribution of this potential indicates an efficient magnetic circuit, while imbalances can reduce motor efficiency. Figure 7 demonstrates a uniform flux line distribution. Magnetic flux density (*B*) indicates the efficiency of the magnetic materials in the motor's magnetic circuits. Excessively high *B* values suggest the material is approaching magnetic saturation, increasing iron losses, while low *B* values indicate underutilization, reducing power efficiency. Operating in the knee region of the $B-H$ curve ensures optimal motor performance (Avsar et al., 2024b). As seen in Figure 8, the magnetic flux densities lie in the knee region of the *B-H* curve of the utilized steel material, indicating maximum efficiency without saturation. The current densities in the windings are shown in Figure 9, with an average current density of 3.7 A/mm^2 and a maximum of 4.41 A/mm^2, demonstrating that the motor operates within safe limits even under high loads.

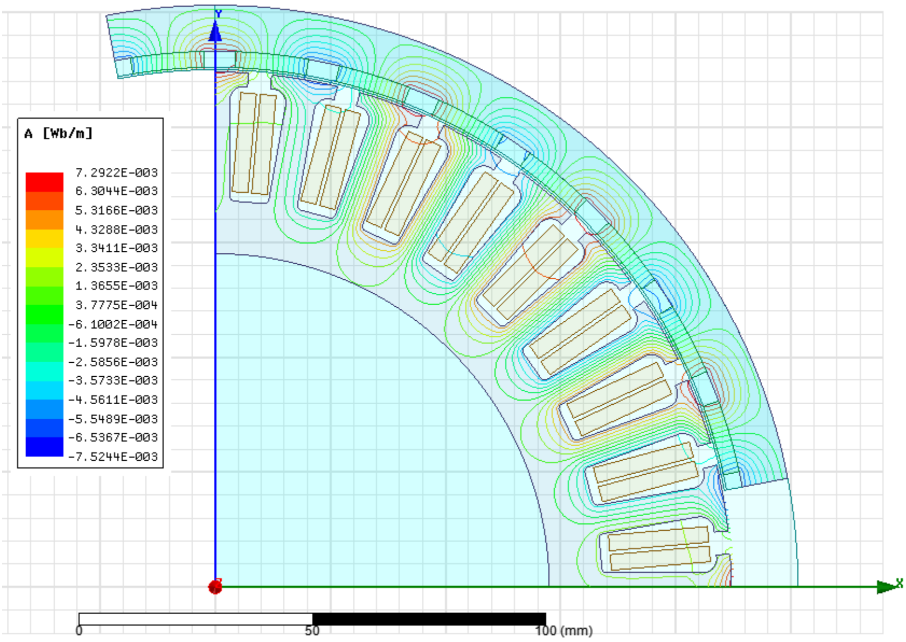

Figure 7. Magnetic vector potential (A:Wb/m)

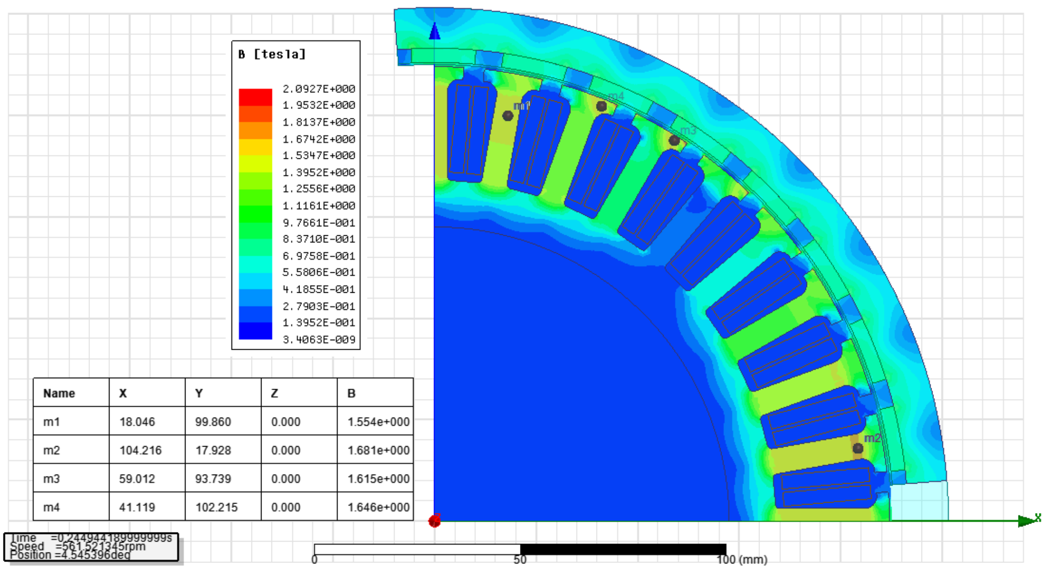

Figure 8. Magnetic flux density (B:Tesla)

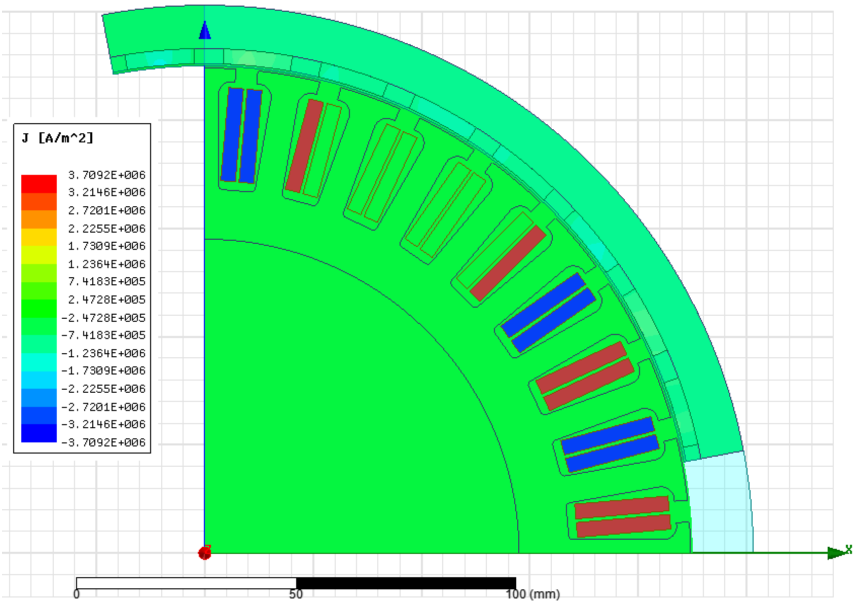

Figure 9. Electric current density (J:A/m^2)

Figure 10 shows the motor's RMS current as 31.9 A, while Figure 11 indicates a nominal efficiency of 90.5%. The output torque graph in Figure 12 reveals a torque ripple of ±4.3 Nm, equivalent to 11.83% of the nominal output torque of 36.35 Nm, which is within acceptable limits for BLDC motors.

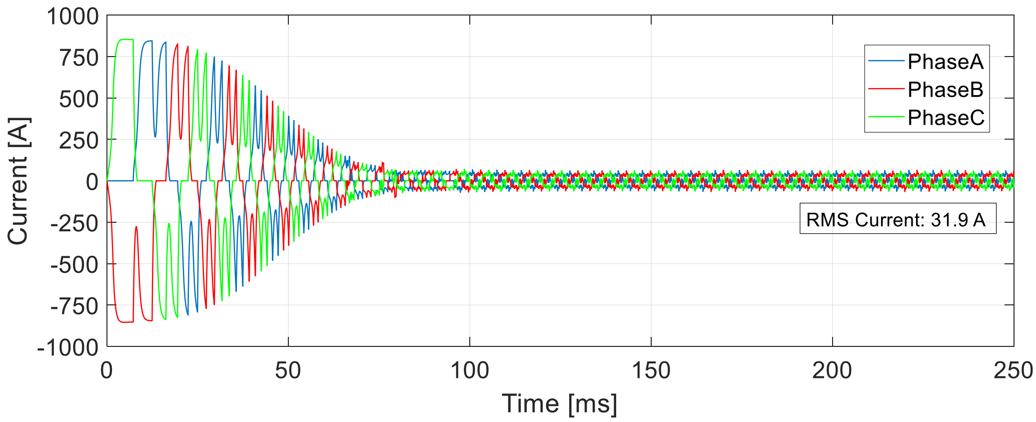

Figure 10. Time-current graph

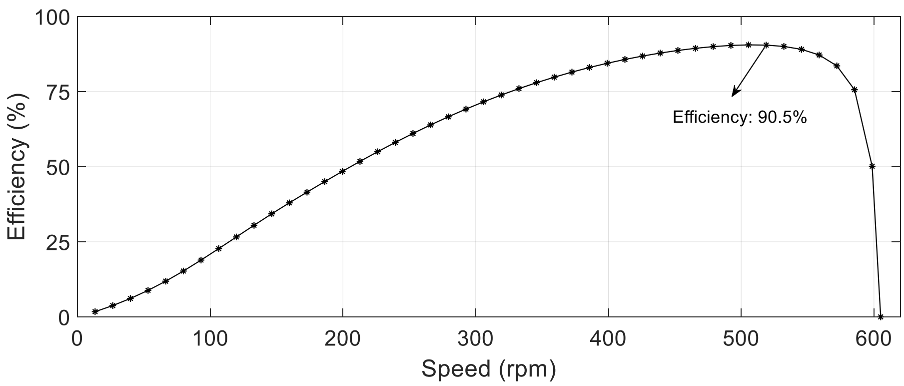

Figure 11. Speed-efficiency graph

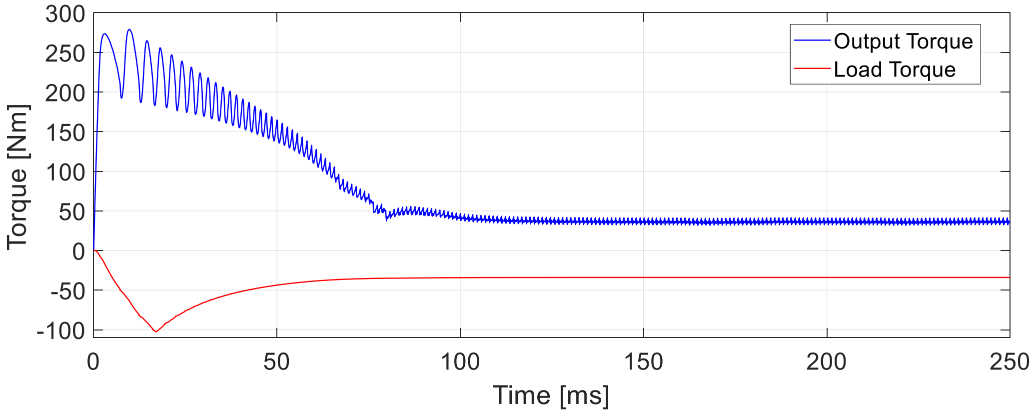

Figure 12. Time-torque graph

In electric motors, windings experience the highest temperatures. Since the magnets are not in direct contact with the windings and rotate with the rotor, their temperatures remain lower than the stator windings. Thus, the maximum winding temperature reflects the motor's maximum internal temperature (Soyaslan, 2020).

Thermal analyses were conducted by linking Ansys Maxwell and Ansys Workbench (Bazazian, 2022). Results obtained from the Ansys Maxwell 2D module were transferred to the Steady-State Thermal module in Ansys Workbench. Thermal properties of materials were defined, contact surfaces specified, and heat generation data and mesh structures imported from Maxwell. The ambient temperature was set to 40°C for the analysis. At full load, the motor reached a steady-state temperature, with results shown in Figure 13. Maximum temperatures of 65.79°C for the windings and 51.75°C for the magnets indicate safe thermal operation.

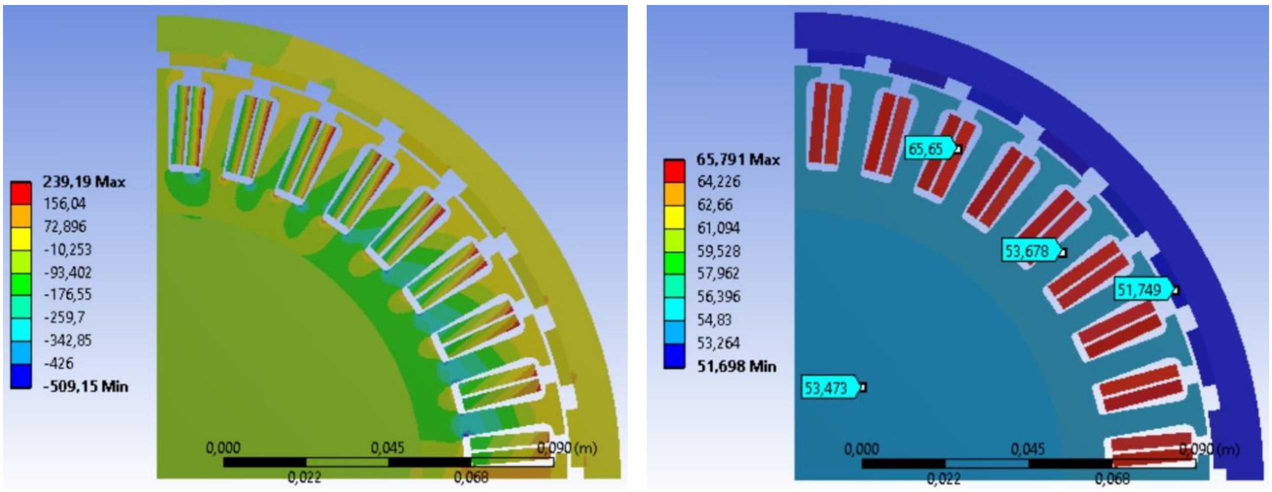

a) b)

Figure 13. a) Directional heat flux, b) Temperature distribution

3.1 Production and Test Results

Following the electromagnetic and thermal validations, the 3D design and technical drawing for direct wheel drive were created, as shown in Figure 14. An aluminum hub was used between the motor shaft and stator core. Slots for the magnets were machined into the rotor via wire erosion, ensuring consistent spacing between magnets. The motor's nameplate values are provided in Table 4, and production images of the motor components are displayed in Figure 15.

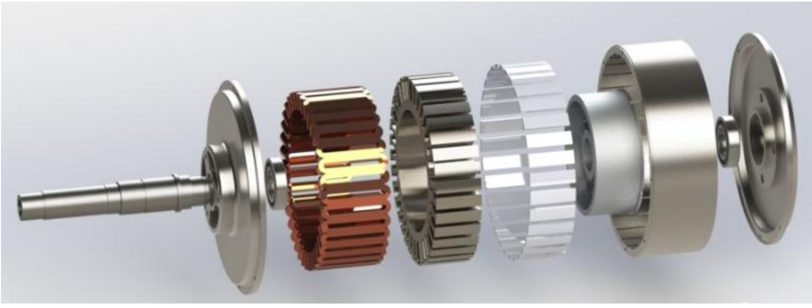

a)

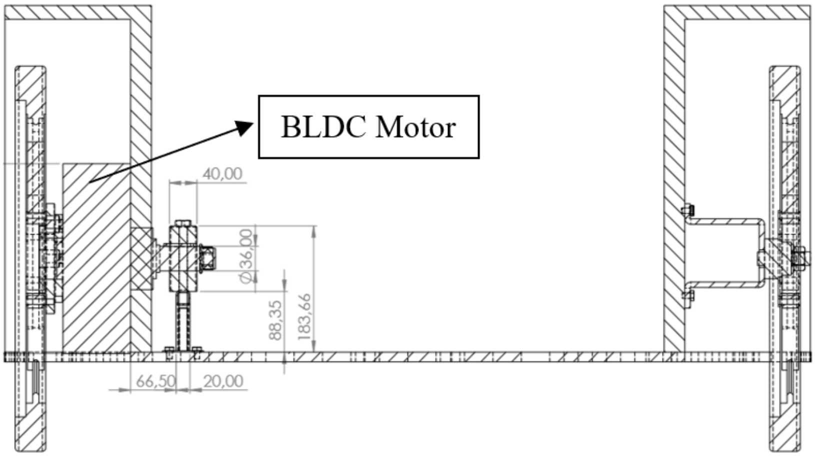

b)

Figure 14. a) 3D model of the BLDC motor, b) Placement of the motor on the EV

Table 4. BLDC motor nameplate values

Parameter	**Value**
Power (kW)	2
Voltage (V)	72
Efficiency (%)	90.5
Rated torque (Nm)	36.35
Rated speed (rpm)	561.5
Rated rms current (A)	31.9
Slot number	36
Pole number	32
Winding type	Double layer, Y
Magnet type	N40SH
Magnet thickness (mm)	3.5
Stator material	M350-50A
Output diameter (mm)	253
Stack length (mm)	55

Figure 15. Production of the motor parts

After manufacturing the motor, load tests were conducted on the test bench shown in Figure 16. The test results were compared with the analysis results, demonstrating agreement in Figure 17. Finally, the motor mounted on the electric vehicle is shown in Figure 18. Track tests confirmed the vehicle's operation at expected current values based on road slope. The test results showed that the nominal efficiency value matched the analysis results and was found to be 91%. Also it has been observed that the motor remained within its thermal limits under full load conditions. The differences between the test results and the analysis results stem from the sensitivity of the experimental setup. The small deviations in the obtained results are evaluated within the defined acceptable tolerance ranges.

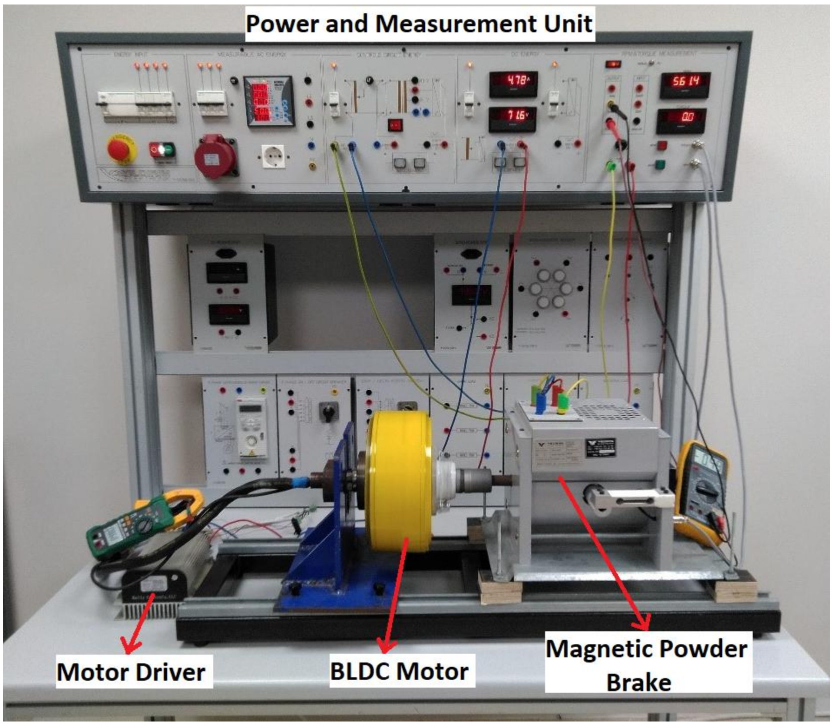

Figure 16. Motor loading tests

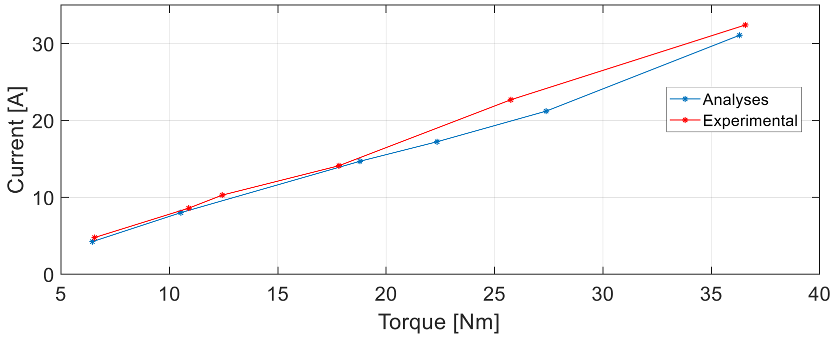

Figure 17. Comparison of analysis and test results

Figure 18. EV with BLDC motor mounted

4. CONCLUSIONS

This study presented the design, production, and validation of a 2 kW outer rotor BLDC motor specifically developed for light electric vehicle applications. The motor was integrated into the vehicle's wheel rim, optimizing weight distribution and improving system efficiency. A dynamic model of the vehicle was constructed to determine the required motor specifications, taking into account the vehicle's characteristics and predefined racetrack conditions. The motor was designed with a 36/32 slot-pole ratio, and the stator tooth tip gap was optimized to minimize cogging torque and improve overall motor performance. Analytical and 2D finite element analyses validated the design, demonstrating that the average magnetic flux density and current density values were kept within safe operational limits. Additionally, parametric optimization yielded an optimal stator tooth tip gap of 5 mm, effectively reducing cogging torque. Thermal analysis confirmed the motor's capability to operate within acceptable temperature ranges, with maximum stator winding temperatures of 65.79 °C and magnet temperatures of 51.75 °C under full load conditions.

Experimental tests of the prototype motor corroborated the analytical and simulation results, achieving a peak efficiency of 90.5% and a rated torque of 36.35 Nm. Torque ripple and temperature performance were within acceptable limits, ensuring reliability and smooth operation. The study highlights the importance of integrating electromagnetic, mechanical, and thermal optimization techniques in motor design to enhance efficiency and performance in light electric vehicle applications. Future work could explore advanced control strategies and alternative cooling solutions to further optimize the performance of outer rotor BLDC motors in similar applications. With advanced control techniques, motor operation can be made more efficient and quieter. These techniques optimize the motor's torque and speed in real-time, minimizing unwanted vibrations and acoustic noise. Additionally, cooling systems can reduce the motor sizes, and current densities can be improved. These advancements enhance the motor's thermal management, allowing it to operate safely at higher current densities while maintaining optimal temperatures, thus enabling more compact and powerful motor designs for high-performance applications such as electric vehicles. This research contributes to the development of compact, high-efficiency motor solutions, paving the way for innovative designs in the electric vehicle industry.

5. ACKNOWLEDGEMENTS

The authors would like to thank to Sakarya University of Applied Sciences, SUBU-TETRA Electromobile Team and its members for their support.

6. CONFLICT OF INTEREST

Authors approve that to the best of their knowledge, there is not any conflict of interest or common interest with an institution/organization or a person that may affect the review process of the paper.

7. AUTHOR CONTRIBUTION

Mücahit SOYASLAN contributed to the Determining the concept and/or design process of the research. Mücahit SOYASLAN contributed to the Management of the concept and/or design process of the research. Mohamad BAZAZIAN contributed to the Data Collection. Mücahit SOYASLAN, Mohamad BAZAZIAN, and Osman ELDOĞAN contributed to the Data analysis and interpretation of the results. Mücahit SOYASLAN contributed to the Preparation of the manuscript. Mohamad BAZAZIAN and Osman ELDOĞAN contributed to the Critical analysis of the intellectual content. Mücahit SOYASLAN, Mohamad BAZAZIAN, and Osman ELDOĞAN contributed to the Final approval and full responsibility.

8. REFERENCES

Akar M., Eker M., Akın F., BLDC motor design and application for light electric vehicle. Afyon Kocatepe University, Journal of Science and Engineering 21.2, 326-336, 2021.

Aliyadin A. Z., Purwadi A., Hidayat S., Performance Analysis and Design of 250 Watt Outer Rotor BLDC Motor for Urban Electric Bicycles, 2022 7th International Conference on Electric Vehicular Technology (ICEVT), Bali, Indonesia, 2022, pp. 195-199, doi: 10.1109/ICEVT55516.2022.9925011.

Anuja T.A., Doss M.A.N., Reduction of Cogging Torque in Surface Mounted Permanent Magnet Brushless DC Motor by Adapting Rotor Magnetic Displacement. Energies 14 (10), 2861, 2021. https://doi.org/10.3390/en14102861.

Anuja T.A., Doss M.A.N., Senthilkumar R., Rajesh K.S., Brindha R., Modification of Pole Pitch and Pole Arc in Rotor Magnets for Cogging Torque Reduction in BLDC Motor, IEEE Access, vol. 10, pp. 116709-116722, 2022. doi: 10.1109/ACCESS.2022.3217233.

Avsar Y., Fenercioglu A., Soyaslan M., Design Optimization of PM Synchronous Motor: Rail Mounted Belt Drive Elevator Systems, IEEE Transactions on Industry Applications, vol. 60, no. 1, pp. 301-311, Jan.-Feb. 2024b. doi: 10.1109/TIA.2023.3311781.

Avsar, Y., Soyaslan, M., & Fenercioglu, A. PMSM Design for Elevators: Determination of the Basic Topology Affecting Performance. The Eurasia Proceedings of Science Technology Engineering and Mathematics, 28, 342-351, 2024a. https://doi.org/10.55549/epstem.1523527

Bazazian, M., Design of an outer rotor brushless dc motor used in electric vehicles, Master Thesis. Dept. of Mechatronics Eng., Sakarya University of Applied Sciences, Graduate Education Institute, Sakarya, 2022.

Cabuk, A. S., Saglam, S., & Ustün, Ö., Investigation on efficiency of in-wheel BLDC motors for different winding structures. Journal of the Faculty of Engineering and Architecture of Gazi University, 34(4), 1975-1985, 2019.

Cagıslar A. S., İn S., Tiryaki H., Effects of Magnet Type and Thickness on Outer Rotor Brushless Direct Current Motor Designed by Calculating the Required Motor Power for an Electric Vehicle Prototype. Erzincan University Journal of Science and Technology 13(3), 1025-1041, 2020. https://doi.org/10.18185/erzifbed.707837.

Chawrasia S.K., Das A., Chanda C.K., Banerjee S., Design, analysis and comparative study of Hub motor for an electric bike. Michael Faraday IET International Summit 2020a MFIIS, pp. 242–247, 2020. https://doi.org/10.1049/icp.2021.1179.

Doss M., Mohanraj K., Vakesan K., Karthik K., Reduction of Cogging Torque by Adapting Bifurcated Stator Slots and Minimization of Harmonics and Torque Ripple in Brushless DC Motor, International Journal of Power Electronics and Drive Systems (IJPEDS), 7(3), 781, 2016. https://doi.org/10.11591/ijpeds.v7.i3.pp781-789.

Gürdal O., Elektrik Makinalarının Tasarımı, Atlas Yayın Dağıtım, İstanbul, 2001.

Hussain M., Ulasyar A., Sheh Zad H., Khattak A., Nisar S., Imran K., Design and Analysis of a Dual Rotor Multiphase Brushless DC Motor for its Application in Electric Vehicles, Eng. Technol. Appl. Sci. Res., vol. 11, no. 6, pp. 7846–7852, Dec. 2021.

Jhankal T., Design and Cogging Torque Reduction of Radial Flux Brushless DC Motors with Varied Permanent Magnet Pole Shapes for Electric Vehicle Application, Transactions on Energy Systems and Engineering Applications, 4(2), 1-13, 2023. https://doi.org/10.32397/tesea.vol4.n2.535.

Karthick K., Ravivarman S., Samikannu R., Vinoth K., Sasikumar B., Analysis of the Impact of Magnetic Materials on Cogging Torque in Brushless DC Motor, Advances in Materials Science and Engineering, 2021, 1-10. https://doi.org/10.1155/2021/5954967.

Kim Y., Yang B., Kim C., Noise Source Identification of Small Fan-BLDC Motor System for Refrigerators," International Journal of Rotating Machinery, 2006(1). https://doi.org/10.1155/ijrm/2006/63214.

Krasopoulos C.T., Beniakar M.E., Kladas A.G., Velocity and Torque Limit Profile Optimization of Electric Vehicle Including Limited Overload, IEEE Transactions on Industry Applications, vol. 53, no. 4, pp. 3907-3916, July-Aug. 2017, doi: 10.1109/TIA.2017.2680405.

Lee B.-C., Song C.-H., Kim D.-H., Kim K.-C., Study on Process Derivation and Characteristic Analysis for BLDC Motor Design Using Dual Rotor Structure with High Torque Density. Energies 2020, 13, 6745. https://doi.org/10.3390/en13246745.

Leitner S., Gruebler H., Muetze A., Cogging Torque Minimization and Performance of the Sub-fractional hp BLDC Claw-pole Motor, IEEE Transactions on Industry Applications, 55(5), 4653-4664, 2019. https://doi.org/10.1109/tia.2019.2923569.

Mandasari D., Design and Optimization of Brushless DC Motor for Electric Boat Thruster, Evergreen, 10(3), 1928-1937, 2023. https://doi.org/10.5109/7151773.

Minh D., Quoc V., Huy P., Efficiency Improvement of Permanent Magnet BLDC Motors for Electric Vehicles," Engineering Technology & Applied Science Research, 11(5), 7615-7618, 2021. https://doi.org/10.48084/etasr.4367.

Murali, N., Ushakumari, S., Mini, V. P., & Varghesee, A. T., Sizing and Performance Analysis of an Electric Motor in an E-rickshaw. IEEE International Conference on Power Systems Technology (POWERCON) (pp. 1-6), Sep., 2020.

Murat N., Ushakumari S., Mini V.P., Varghesee A.T., Sizing and Performance Analysis of an Electric Motor in an E-rickshaw, 2020 IEEE International Conference on Power Systems Technology (POWERCON), pp. 1-6, Sept. 2020.

Niessen F., Winding Scheme Calculator, Erişim: 31 Ekim 2019, http://www.bavaria-direct.co.za/scheme/calculator/.

Ocak C., Tarimer I., Dalcali A., Uygun D., Investigation effects of narrowing rotor pole embrace to efficiency and cogging torque at PM BLDC motor. TEM Journal 5(1), 25, 2016.

Ozupak Y. Efficiency analysis of BLDC motor for variable magnetic field. MANAS Journal of Engineering,10(1):105-109, 2022. doi:10.51354/mjen.1097668

Ozupak, Y., & Çınar, M. Design and Co-Analysis of A Permanent Magnet Brushless DC Motor By Using Clonal Selection Principle Based Wound Healing Algorithm and Ansys-Maxwell. Gazi University Journal of Science Part A: Engineering and Innovation, 10(4), 499-510, 2023. https://doi.org/10.54287/gujsa.1371904

Rupam, S. Marwaha, Mitigation of Cogging Torque for the Optimal Design of BLDC Motor, IEEE 2nd International Conference On Electrical Power and Energy Systems (ICEPES), Bhopal, India, pp. 1-5, 2021, doi: 10.1109/ICEPES52894.2021.9699544.

Smółka, K. and Firych-Nowacka, A., Comparison of the design of 3-pole bldc actuators/motors with a rotor based on a single permanent magnet. Sensors, 22(10), 3759, 2022. https://doi.org/10.3390/s22103759

Soyaslan M., Avşar Y., Fenercioğlu A., Eldoğan O., Cogging Torque Reduction in External Rotor PM Synchronous Motors by Optimum Pole Embrace, 3rd International Symposium on Multidisciplinary Studies and Innovative Technologies (ISMSIT), Ankara, Turkey, 2019, pp. 1-4, doi: 10.1109/ISMSIT.2019.8932915.

Soyaslan M., Design of an External Rotor Permanent Magnet Synchronous Motor for Elevator Traction Systems, PhD Thesis, Dept. of Mechatronics Eng., Sakarya University, Institute of Natural Sciences, Sakarya, 2020.

Soyaslan, M., External Rotor BLDC Motor Design for a Light Electric Vehicle: 24 Slot/22 Pole Combination, 18th Conference on Electrical Machines, Drives and Power Systems (ELMA), Varna, Bulgaria, pp. 1-4, 2023, doi: 10.1109/ELMA58392.2023.10202463

Tosun, O., Serteller, N.F.O., The Design of the Outer-Rotor Brushless DC Motor and an Investigation of Motor Axial-Length-to-Pole-Pitch Ratio. Sustainability 2022, 14, 12743. https://doi.org/10.3390/su141912743.

Vadde A., Sachin S., Influence of Rotor Design in BLDC Motor for Two-Wheeler Electric Vehicle, 1st International Conference on Power Electronics and Energy (ICPEE), Bhubaneswar, India, 2021, pp. 1-6, doi: 10.1109/ICPEE50452.2021.9358520.

Zuki, N. A. M., Othman, R. N. F. K. R., Ahmad, S. R. C., & Shukor, F. A. A., Consideration of various constants in double stator permanent magnet brushless DC motor, International Journal of Applied Electromagnetics and Mechanics 63.1, 1-17, 2020.